Shear-Induced Deformation and Desorption of Grafted Polymer Layers

M. Aubouy, J.L. Harden, M. Cates

J. Phys. II France 6 (1996) 969–984 JULY 1996, PAGE 969

Shear-Induced Deformation and Desorption of Grafted Polymer Layers

M. Aubouy ([1,2,3,*]), J.L. Harden ([3,4]) and M.E. Cates ([3])

([1]) Laboratoire de Physique de la Matière Condensée ([**]), Collège de France,
11 place Marcelin Berthelot, 75231 Paris Cedex 05, France
([2]) Laboratoire de Reconnaissance des Matériaux dans leur Environnement ([***]),
Université de Marne-la-Vallée, 2 rue du Promontoire, 93166 Noisy-le-Grand Cedex, France
([3]) Department of Physics and Astronomy, University of Edinburgh,
James Clerk Maxwell Building, King's Buildings, Mayfield Road, Edinburgh EH9 3JZ, UK
([4]) Cavendish Laboratory, Cambridge University, Madingley Road, Cambridge CB3 OHE, UK

(Received 29 December 1995, received in final form 1 April 1996, accepted 4 April 1996)

PACS.68.10.-m – Fluid surfaces and fluid-fluid interfaces
PACS.82.70.-y – Disperse systems
PACS.36.20.-r – Macromolecules and polymer molecules

Abstract. — We describe the behaviour of grafted polymer layers in strong solvent shear flows within a model where only a subset of chains are exposed to the flow (hence to the tension arising from hydrodynamic drag forces), leaving the remainder protected. We show that for quite small values of the shear rate, $\dot{\gamma}$, the system reaches a self-regulating state where the lowest possible fraction of grafted chains is exposed to the flow. This brings quantitative corrections to previous models (all based on the assumption that the chains behave alike) which correspond to a higher susceptibility of the layer to shear fields: the onset of significant swelling occurs at a lower shear rate and at high shear rates the asymptotic value of the relative swelling is somewhat larger. Furthermore we find that the behaviour of the layer strongly depends on both the index of polymerisation of the chains and the grafting density. In particular, for thick brushes, our model predicts a discontinuous (first order) swelling transition at a critical shear rate. The model is used to study the rate of desorption of individual chains grafted *via* compact end-stickers and insoluble polymer blocks. In both cases, there is a strong increase in desorption at the swelling transition. For the case of end-sticker grafting, we find the desorption rate $\mathcal{R}$ obeys $\mathcal{R} \sim \dot{\gamma}^3$ for large shear rates; while in the case of diblock grafting, we find that the barrier height to desorption is a strong function of shear rate, leading to an exponentially enhanced desorption rate for large $\dot{\gamma}$: $\mathcal{R} \sim e^{\dot{\gamma}\tau_0}$

1. Introduction

Polymers at interfaces show remarkable properties from both a scientific and technological point of view and have been the subject of numerous recent studies. One of the most investigated

(*) Author for correspondence (e-mail: Aubouy@ext.jussieu.fr)
(**) URA n° 792 CNRS
(***) UPR n° 343 CNRS

situations is preferential adsorption, when polymer chains are grafted by one end to a repulsive surface. At sufficiently high coverage, the chains stretch away from the interface to avoid excluded volume interactions, this elongation being counterbalanced by an elastic restoring force of entropic origin. The resulting layer formed from these stretched polymers is often referred to as a polymer brush. Both scaling and self-consistent field approaches have been used to model the static properties of polymer brushes, which are now well understood [1,2].

Polymer brushes in good solvent conditions are rather diffuse and soft structures, and hence are very sensitive to external perturbations. In particular, there is experimental evidence that polymer brushes *swell* in sufficiently high shear-rate solvent flows [3,4]. This behaviour was rationalized by Barrat [5], who considered carefully the Rabin-Alexander model [6] of the polymer brush deformation in response to applied boundary shear forces. In this approach, the response of the layer to a fixed shear force $F_{\|}$ applied to the free end of each grafted chain was investigated by assuming that all chains behave alike and are uniformly stretched (the Alexander-de Gennes ansatz [7,8]), and by making use of the Pincus scheme [9] for describing a chain under traction. The result is a non-linear increase of the thickness of the layer as a function of the applied force. However, quantitative comparison with experiment is difficult since the shear rate $\dot{\gamma}$ is the experimentally relevant parameter, whereas the effective boundary shear force $F_{\|}$ is unknown. Recently, a more complete scaling model was proposed [10] which allows non-uniform stretching of the chains [11,12] and calculates, in a mutually consistent manner, the deformation of the layer and the solvent velocity profile. The results of reference [10] can be interpreted in terms of a (simplified) "quasi-monoblock" picture where each chain is composed of a tilted, linear string of small Pincus blobs terminated by a larger blob of size ξ_{end}, typically of order the average separation between grafting points, ξ_0, when the shear rate is not too large. The shear flow, which only penetrates a distance ξ_0 into the layer, exerts a drag force on each chain $F_{\|} \cong 6\pi\eta\dot{\gamma}\xi_0^2 \cong \dot{\gamma}\tau_0\, k_B T/\xi_0$, where η is the solvent viscosity, $k_B T$ is the thermal energy and $\tau_0 \cong \eta\xi_0^3/(k_B T)$ is the characteristic Zimm relaxation time of a blob of the unperturbed brush. The relative swelling of the brush as a function of the relevant parameter $\dot{\gamma}\tau_0$ shows an asymptotic value of $\cong 25\%$ for $\dot{\gamma}\tau_0 \gg 1$, in accordance with Barrat's calculation [5]. However, a rough comparison between theory and experiment shows a discrepancy of one order of magnitude in the value of $\dot{\gamma}$ required to produce the experimentally reported brush swelling of $\cong 20\%$. As pointed out by the authors of reference [10], an inherent limitation of their approach remains the Alexander-de Gennes ansatz [7,8] which assumes that all chains behave alike. This approximation is appropriate when considering properties which are not sensitive to the detailed structure of the layer, but several important features are absent. For equilibrium brushes, self-consistent field calculations [13,14] show that the free ends are in fact distributed in the whole layer, rather than concentrated at its extremity. This means that the effective number of chains per unit surface in the outer fringe of the brush is lower than the value $\sigma = a^2/\xi_0^2$ at the grafting surface, and we thus might expect a decrease in the value of $\dot{\gamma}\tau_0$ at the onset of swelling (since $\dot{\gamma}\tau_0 \sim \sigma^{-3/2}$).

An interesting aspect of this problem, in terms of the underlying physics, is the possibility that the system might respond to shear flows by exposing a subset of chains to a higher tension, leaving the remainder protected from flow, rather than exposing all of them to an equal but lower tension. This could lead to a modified flow response, which we wish to explore in this paper. Such effects could be particularly important in processes like desorption, which may depend critically on the state of the most highly deformed chains. Unfortunately, a complete theory of the brush response to shear flows involves allowing all possible configurations for the grafted chains, and therefore is a formidable task. Furthermore, self-consistent field models are based on arguments which are very sensitive to any perturbation of the equilibrium structure and cannot be easily generalized.

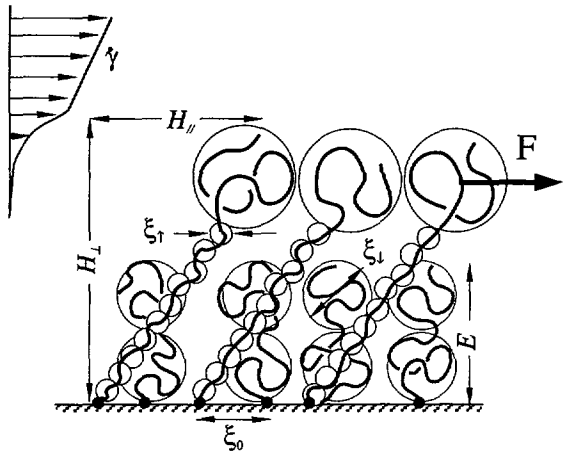

Fig. 1. — Sketch of the dual-chain brush configuration. A fraction f of the chains are extended and tilted by the shear flow; we assume that they form a quasi-monoblock layer of dragged chains. The remaining fraction $1 - f$ lie deeper in the adsorbed layer, where the flow is screened; we assume that they form a quiescent Alexander-de Gennes brush in the volume left unoccupied by the dragged ones.

In the present paper, we therefore consider a simplified "dual-chain" model in which only two types of chains are present (see Fig. 1): a fraction f of the chains which are extended and tilted by the shear flow (hereafter called the "dragged" chains), and the remaining fraction $1 - f$ which lie deeper in the adsorbed layer, where the flow is screened (hereafter called the "quiescent" chains). We assume, following reference [10], that the dragged chains form a quasi-monoblock-like layer, while the screened fraction form a quiescent Alexander-de Gennes type brush amid the lower sections of the strongly deformed chains. This model is clearly oversimplified, but goes part of the way to relaxing the constraint that all chains behave alike. We believe it may offer some useful qualitative insights into the full problem.

Due to a conservation law for the shear stress arising from flow (the total shear force acting on the layer *per unit surface area* is independent of chain conformations), each of the dragged chains experiences a force $F_{||} \cong \eta\dot{\gamma}/(f\sigma)$. The dragged chain fraction is not fixed at the onset, but rather is determined through the minimization of an effective free energy, subject to suitable constraints. The deformation of the dragged chains in response to $F_{||}$ competes with excluded volume and chain elasticity effects throughout the brush to determine the dependence of f on the applied shear flow, and the resulting structure of the grafted layer as a whole. This process is analysed in detail in Section 2. We will show that with increasing shear rate, fewer chains participate in the upper layer, with f decreasing towards a low, self-regulating, limiting value at high shear rates. As for the global properties of the layer, a somewhat higher susceptibility of the brush to shear fields is predicted than in the one-component Alexander-de Gennes-type picture presented in references [5,10]: the onset of significant swelling occurs at a lower shear rate and the asymptotic value of the relative swelling is larger. These predictions offer quantitative but not qualitative corrections to previous models. In some circumstances, however, f may undergo a (formally discontinuous) "jump" as the shear rate is increased. Another qualitative difference is that in our approach, the behaviour of the layer under shear flows depends strongly on the degree of polymerisation N of the chains; whereas previous models were either independent of N [5] or weakly dependent on N [10].

In addition to the swelling effect there are some other properties which may depend strongly on the details of shear-induced deformation. One such case arises in the analysis of the desorption rate for chains in a grafted layer subject to shear flows, which we explore in some detail in Section 3. (We are unaware of previous discussions of this subject even within the simplest, one-component brush models.) Brush formation is generally caused by the preference for one extremity of the chain to associate with the grafting surface. Experimentally, the anchoring end group can be a strong sticker (*e.g.* an adsorbed zwitterionic group or a weak covalent bond), or a section of insoluble polymer of different chemistry (*e.g.* a diblock copolymer in selective solvent). In all cases, the work of detachment of the anchor ΔU must be large compared to $k_B T$ to overcome the osmotic interaction between the chains in the brush (for which we presume the solvent is good). The desorption of a grafted chain occurs by the detachment of its anchoring end, followed by the expulsion of the chain from the layer [15]. In the absence of flow, detachment is a thermally activated process involving, due to osmotic pressure effects, a high potential barrier ΔU, and so may be extremely slow. The application of a shear flow, which in effect puts the chains under an external tension (arising from hydrodynamic drag forces), can strongly increase the desorption rate. In Section 3 this shear-enhanced desorption process is analysed in the context of our dual-chain model for both the strong sticker and diblock copolymer grafting mechanisms. The results for the one-component Alexander-de Gennes-type brush are included as a limiting case. (Hence the reader interested in desorption kinetics but not in the dual-chain model can formally set $f = 1$ in Sect. 3.) Section 4 contains our conclusions.

2. Deformation of a Polymer Brush Under Shear Flows

In this section, we analyse the behaviour of the dual-chain model brush described in the Introduction, and depicted in Figure 1. The brush is subject to hydrodynamic drag forces which we assume to affect only the outermost blobs of the fraction f of the dragged chains. As discussed in the Introduction, each chain supports a force $F_{\|} \cong \eta\dot{\gamma}/(f\sigma)$. The total drag force per unit area which must be supported is determined by the solvent shear gradient outside the brush, and is f-independent. (The value of f does however affect the displacement of the upper surface of the layer and hence the work done by the drag.) Following reference [5], we treat the drag forces as if they arose through an external *thermodynamic* perturbation, and minimize the resulting effective free energy within a suitable ensemble. (This would not be possible if the total drag force per unit area depended of f.)

The effective free energy $\mathcal{F}$ of this system is the sum of an osmotic contribution, $\mathcal{F}_{\rm osm}$, involving excluded volume interactions, and an elastic contribution, $\mathcal{F}_{\rm el}$, involving the conformations of the deformed coils. These are estimated by representing the chains as linear strings of non-overlapping excluded-volume blobs (Pincus blobs [9]). The typical blob sizes of the dragged and protected chains are, respectively, $\xi_{\uparrow}$ and $\xi_{\downarrow}$. In this approach, the elasticity of a stretched chain may be computed as if it was a Gaussian string of Pincus blobs [9]. This leads to an elastic energy per unit area of the form

$$\mathcal{F}_{\rm el} \cong \frac{2}{5} k_B T \frac{\sigma}{a^2 N^{3/2}} \left(f L^{5/2} + (1-f) E^{5/2} \right) \tag{1}$$

where the first and second terms are the contributions of the dragged (upper) and quiescent (lower) layers, and where we have neglected the contribution from the single larger blob at the extremity of the upper layer. In this equation, $L = (H_{\|}^2 + H_{\perp}^2)^{1/2}$ is the magnitude of the end-to-end vector $(H_{\|}, H_{\perp})$ of a dragged chain, E is the end-to-end distance of an untilted, protected chain, and N is the polymerization index (the same for all chains). In the spirit of references [5,6,10], the excluded volume interactions are computed as if the layer was a fluid of

independent blobs of two different sizes. To lowest order in a virial expansion, this gives three terms in $\mathcal{F}_{\rm osm}$ corresponding to the self interactions ($\uparrow\uparrow$ and $\downarrow\downarrow$) and the mutual term ($\uparrow\downarrow$):

$$\begin{aligned}
\mathcal{U}_{\uparrow\uparrow} &\cong 2k_{\rm B}T\frac{\sigma^2}{N^3}f^2 v_{\uparrow\uparrow}(L/a)^5/(H_\perp/a) \\
\mathcal{U}_{\downarrow\downarrow} &\cong 2k_{\rm B}T\frac{\sigma^2}{N^3}(1-f)^2 v_{\downarrow\downarrow}(E/a)^4 \\
\mathcal{U}_{\uparrow\downarrow} &\cong 4k_{\rm B}T\frac{\sigma^2}{N^3}f(1-f)v_{\uparrow\downarrow}(E/a)^{5/2}(L/a)^{5/2}
\end{aligned} \tag{2}$$

where $v_{\uparrow\uparrow}$, $v_{\downarrow\downarrow}$, and $v_{\uparrow\downarrow}$ denote the respective excluded volume parameters. Two identical blobs behave as hard spheres, thus $v_{\uparrow\uparrow} = \xi_\uparrow^3$ and $v_{\downarrow\downarrow} = \xi_\downarrow^3$. (We suppress various order unity prefactors here and below). As shown by Lapp *et al.* [16], this is not the case for two blobs of different sizes, and we should instead write $v_{\uparrow\downarrow} = \xi_\uparrow^3(\xi_\downarrow/\xi_\uparrow)^{5/3}$. (The idea is that the excluded volume between a small coil and a large one is equal to the volume of the small one multiplied by the number of times it can be replicated in the large one.) Inserting these into equations (2) and using the Pincus scheme to write $\xi_\uparrow$ and $\xi_\downarrow$ in terms of L, E, N, and a, we find an osmotic contribution to the free energy of the form

$$\mathcal{F}_{\rm osm} \cong 2k_{\rm B}T\sigma^2\frac{N^{3/2}}{a^2}\left(\frac{(1-f)^2}{E^{1/2}} + \frac{f^2L^{1/2}}{H_\perp} + 2\frac{f(1-f)L^{1/2}}{H_\perp}\right) \tag{3}$$

The behaviour of the system is now given by the minimization of the pseudo thermodynamic potential $\mathcal{G} = \mathcal{F} - f\sigma F_\parallel H_\parallel$, where $\mathcal{F} = \mathcal{F}_{\rm el} + \mathcal{F}_{\rm osm}$ and $F_\parallel \cong \eta\dot\gamma/(f\sigma)$. Using equations (1) and (3), this may be written in a dimensionless form as

$$\tilde{\mathcal{G}} \cong \frac{2}{5}f\ell^{5/2} + \frac{2}{5}(1-f)e^{5/2} + 2\frac{(1-f)^2}{e^{1/2}} + 2f(2-f)\frac{\ell^{1/2}}{h_\perp} - (\dot\gamma\tau_0)h_\parallel \tag{4}$$

where, $\tilde{\mathcal{G}} = a^2\mathcal{G}/(k_{\rm B}TN\sigma^{11/6})$, $h_\perp = H_\perp/L_0$, $h_\parallel = H_\parallel/L_0$, $\ell = (h_\parallel^2 + h_\perp^2)^{1/2}$, $e = E/L_0$, and $L_0 = aN\sigma^{1/3}$, the thickness of a static Alexander-de Gennes brush [17].

Minimization of the pseudo-potential equation (4) with respect to $h_\perp$, $h_\parallel$, e and f results in the following set of four coupled equations

$$\tilde h_\perp^3 = 2\left(1 - \frac{\tilde h_\perp^2}{2\tilde\ell^2}\right) \tag{5}$$

$$\frac{(\dot\gamma\tau_0)}{f(2-f)^{1/2}} = \tilde h_\parallel\tilde\ell^{1/2}\left(1 + \frac{1}{\tilde h_\perp\tilde\ell^2}\right) \tag{6}$$

$$\tilde e = 1 \tag{7}$$

$$10\frac{\tilde\ell}{\tilde h_\perp} - 11\left[\left(\frac{2-f}{1-f}\right)^{1/6}\tilde\ell^{1/2}\right] + \left[\left(\frac{2-f}{1-f}\right)^{1/6}\tilde\ell^{1/2}\right]^6 = 0 \tag{8}$$

written in terms of the rescaled variables

$$\tilde h_\parallel = \frac{h_\parallel}{(2-f)^{1/3}}, \quad \tilde h_\perp = \frac{h_\perp}{(2-f)^{1/3}}, \quad \tilde e = \frac{e}{(1-f)^{1/3}} \tag{9}$$

We have solved these coupled equations numerically as a function of $\dot\gamma\tau_0$.

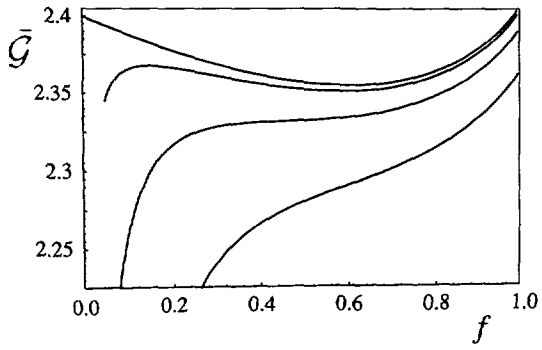

Fig. 2. — Plots of the pseudo thermodynamic potential $\bar{\mathcal{G}}$ *versus* f for different values of the dimensionless shear parameter: $\dot{\gamma}\tau_0$ =0 (highest curve), 0.1, 0.23, 0.4 (lowest curve).

We first note an interesting result that emerges when we consider the solution of these four equations in the zero-flow limit: the fraction f which minimizes the potential is $f_m(\dot{\gamma}\tau_0 = 0) \cong 0.62$. We recover here, using a rather unusual approach, the well-known result that, at equilibrium, the solution $f = 1$ (associated with the Alexander-de Gennes ansatz) is unstable. Rather than finding the true equilibrium state (in which the chain ends are distributed throughout the layer [13, 14]), our model finds the best compromise between excluded volume and stretching within a dual chain description.

The evolution of the system as a function of the shear rate can be understood from Figure 2, where the variation of the pseudo-potential $\bar{\mathcal{G}}$ with f is plotted for different values of the parameter $\dot{\gamma}\tau_0$. As $\dot{\gamma}\tau_0$ is increased from zero, a second minimum appears at $f = 0$ and the original one, $f_m(\dot{\gamma}\tau_0)$, is progressively shifted to lower values. This continues until $(\dot{\gamma}\tau_0) \cong 0.23$, where the original minimum disappears entirely, and the system can, within the approximations so far made, continuously decrease its potential by lowering f to zero. Clearly, however, the layer cannot explore the very low f region due to coverage constraints: for our model to be valid, there must always be enough chains participating in the upper layer to screen the flow from the lower layer, which is presumed quiescent. In practice, this effect will stabilize the system at a nonzero value of f. Let f_{co} denote the crossover fraction, below which the shear flow perturbs the bottom layer. Any perturbation which would lower f below f_{co} will result in the penetration of the flow into the lower layer. In response to this flow, some of the "protected" chains will feel drag forces causing them to stretch and become participants in the upper layer, leading to an increase in f. This argument suggests that, to find the physical value of f, we should choose the value that minimizes our effective potential $\bar{\mathcal{G}}$ subject to the constraint $f \geq f_{co}$.

We now proceed to estimate the crossover value f_{co}, below which the shear flow is not efficiently screened by the upper layer. A rigorous estimate would involve a complete description of the hydrodynamics in the outer portion of the layer and lies beyond the scope of our simple model. A plausible candidate for the crossover fraction is obtained by demanding that the height difference between the upper and lower layers, $H_\perp - E$, is larger than the characteristic hydrodynamic screening length in the upper layer, λ_{sc}. hence we set $f = f_{co}$ when $H_\perp - E \cong \lambda_{sc}$. According to our description, the dragged chains form an Alexander-de Gennes brush, with area grafting density $f\sigma$, exposed to a shear field. A scaling analysis of the hydrodynamics inside these layers is provided by reference [10] and results in an estimate of the screening length as roughly the average lateral separation between chains (*i.e.*

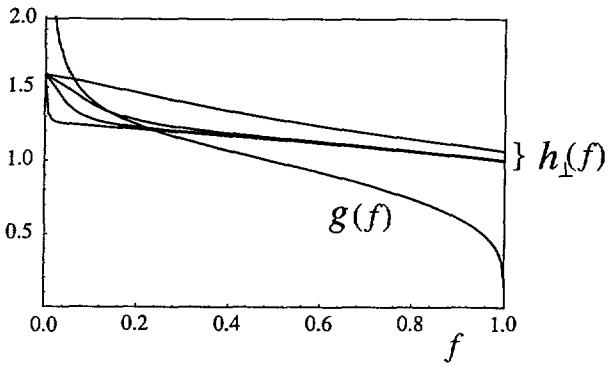

Fig. 3. — Plots of $g(f) = (1-f)^{1/3} + n_b^{-1} f^{-1/2}$ and $h_\perp(f)$ (for different values of the shear parameter: $\dot{\gamma}\tau_0$ =0.01 (lowest curve), 0.1, 0.23, 1 (highest curve)). For a given $\dot{\gamma}\tau_0$, the threshold f_{co} is obtained from intersection of the $g(f)$ and $h_\perp(f)$ curves.

$\lambda_{sc} \cong a(f\sigma)^{-1/2}$ in our case), independent of the shear rate. Using equations (7, 9), the criterion that $H_\perp - E = \lambda_{sc}$ at $f = f_{co}$ can be written as the following implicit equation for f_{co}

$$h_\perp(f_{co}) = (1 - f_{co})^{1/3} + \frac{1}{n_b f_{co}^{1/2}} \tag{10}$$

where $n_b = N\sigma^{5/6}$ is the average number of blobs per chain in the brush at equilibrium, and where $h_\perp(f)$ is obtained from the solution of equations (5, 6). For each value of $\dot{\gamma}\tau_0$, there is a different function $h_\perp(f)$, hence a different crossover value f_{co} (see Fig. 3 for a graphical solution to Eq. (10)). The resulting function $f_{co}(\dot{\gamma}\tau_0)$ monotonically decreases towards an asymptotic value at high shear rates. Both the initial value $f_{co}(\dot{\gamma}\tau_0 = 0)$ and the asymptotic limit strongly depend on n_b, with $f_{co} \sim n_b^{-2}$ in the limit $\dot{\gamma}\tau_0 \gg 1$.

The dependence of the fraction f of dragged chains on the reduced shear rate $\dot{\gamma}\tau_0$ can now be understood from Figure 4, which shows plots of f_{co}, f_m, and f_0 as a function of $\dot{\gamma}\tau_0$. Here we have introduced a quantity f_0 such that $\bar{\mathcal{G}}(f_0) = \bar{\mathcal{G}}(f_m)$; whenever the curve is nonmonotonic (so that a minimum exists at f_m), f_0 denotes the point at which the curve recrosses below the local minimum at f_m as f is decreased. The two points at f_m and f_0 annihilate each other at $\gamma\tau_0 \simeq 0.23$ as mentioned previously; beyond this, the curve is monotonic. (The precise value of $\gamma\tau_0$ is model dependent.) The physical behaviour depends on the relative values of f_0 and f_{co}. A low shear rate, f_{co} is higher than f_0 and so the fraction which minimizes the potential $\bar{\mathcal{G}}$ is simply f_m. As the shear rate is increased, however, f_0 and f_{co} may cross, leading to a situation where f_{co} is lower than f_0. In this case there exists a region at low f, not excluded by our requirement of screening of the quiescent chains (so that the constraint $f \geq f_{co}$ is fulfilled), where the effective potential is lower than its value at the local minimum f_m. Beyond this shear rate, the fraction f which minimizes $\mathcal{G}$ is then given by f_{co}. Thus, f "jumps" discontinuously from f_m to f_{co} at the shear rate for which f_0 and f_{co} coincide. Note that we do not expect any "phase separation" between high-f regions and low-f regions in this situation. This scenario applies so long as n_b is sufficiently large; for small enough n_b, in contrast, f_0 and f_m annihilate before f_{co} can fall below f_0. The division between these regimes is prefactor dependent, but with our choice of prefactors the first scenario applies for all reasonable n_b (*i.e.*, $n_b \geq 4$).

Accordingly, within our model, the discontinuous jump in properties is a generic feature which becomes more and more pronounced as n_b is increased. This is displayed Figure 4,

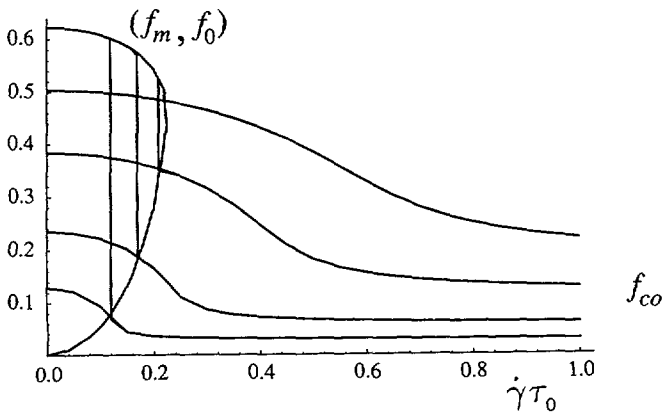

Fig. 4. — Plots of the functions f_{co} (for $n_b = 4$ (highest curve), 5, 7, and 10 (lowest curve)), f_m and f_0 (the fraction below which $\bar{\mathcal{G}}$ is lower than its value at f_m, see Fig. 2) *versus* $\dot{\gamma}\tau_0$. The function f_m (resp. f_0) is the upper (resp. lower) branch of (f_m, f_0). The analysis in the text indicates that the physical fraction f satisfies $f = f_m$ for $f_0 < f_{co}$, after which the fraction becomes $f = f_{co}$.

which shows that the variation of the fraction f with $\dot{\gamma}\tau_0$ is essentially independent of the brush characteristics at low shear rates (below the jump) but strongly dependent on n_b at high shear rates. As n_b is increased, the "jump" occurs at progressively smaller $\dot{\gamma}\tau_0$ and its magnitude increases. We emphasize that the numerical details of the discontinuity as presented above are a consequence of treating our requirement that the quiescent chains be screened as a "hard" constraint: $f \geq f_{co}$. In reality, the constraint is not hard. However, so long as there is some effective free energy penalty (or soft constraint) which prevents the system from attaining $f \ll f_0$, we would still have a sudden jump in behaviour corresponding to a transition from f_m to a new minimum of $\mathcal{G}$ in the neighbourhood of $f = f_0$. Therefore this qualitative aspect does not depend on the details of our arguments concerning screening. Of course, the result may also be a consequence of our adopting the dual chain model; it is possible that in a more detailed treatment the first-order transition would be replaced with a (perhaps fairly sharp) crossover in brush properties.

Figure 5 shows plots of the relative swelling $\delta h = (h_\perp - h_0)/h_0$, where h_0 is the brush height in the zero shear limit, *versus* $\dot{\gamma}\tau_0$ for $n_b = 4, 5, 7$ and 10 (solid curves). For comparison, the one-component Alexander-de Gennes result, obtained by imposing $f = 1$, is also plotted (dashed curve). In both cases we have a non-linear swelling followed by a saturation at large $\dot{\gamma}\tau_0$. There are, however, several notable differences between the two cases. First, qualitatively, our model predicts a stronger dependence of the behaviour of the layer under shear flow on its static characteristics: not only the average size of the blob, ξ_0 (which determines τ_0), but also the average number of blobs in the static layer, n_b, are the key parameters. In contrast, in the previous models the behaviour under shear flow is either entirely determined by the knowledge of τ_0 [5], or only weakly dependent in addition on n_b [10]. Quantitatively, the onset of significant swelling is at a much lower value of $\dot{\gamma}\tau_0$ than in the $f = 1$ case, *e.g.* for $n_b = 7$, $\dot{\gamma}\tau_0 \cong 0.16$ *versus* $\dot{\gamma}\tau_0 \cong 1.0$, though of course the prefactors here are subject to model uncertainties. (It is physically clear that any reduction in f will increase the response to a given shear since, in effect, τ_0 is increased.) Our model also predicts somewhat stronger asymptotic swelling than in the previous Alexander-de Gennes-type approaches (up to 50% *versus* 25%). The latter fact can be directly seen from equations (5, 9) if we realize that the value of the

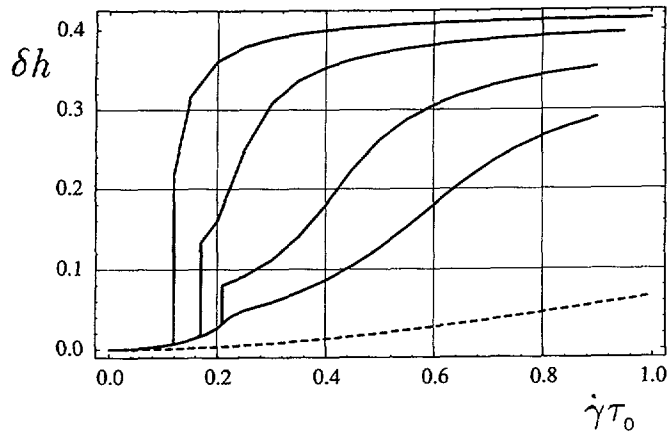

Fig. 5. — Plots of the relative swelling $\delta h = (h_\perp - h_0)/h_0$ *versus* $\dot{\gamma}\tau_0$ for the dual-chain model. The solid lines are for $n_b = 4$ (lowest curve), 5, 7, and 10 (highest curve), while the dashed line is for the case where we impose $f = 1$.

scaled height always asymptotes to $\tilde{h}_\perp \to 2^{1/3}$, implying that $h_\perp \to 2^{1/3}(2-f)^{1/3}$, regardless of the value of f. Since our model predicts small f for $\dot{\gamma}\tau_0 \gg 1$, this leads to enhanced swelling compared to the $f = 1$ case. Similarly, we can understand the earlier onset of swelling directly from equation (6), which can be mapped onto the $f = 1$ case by introducing an effective shear rate parameter:

$$(\dot{\gamma}\tau_0)_{\text{eff}} = \frac{\dot{\gamma}\tau_0}{f(2-f)^{1/2}} \tag{11}$$

Within this mapping, the onset of swelling occurs at $(\dot{\gamma}\tau_0)_{\text{eff}} \cong 1$, regardless of the value of f. However, with decreasing f, this corresponds to a decreasing value of the actual dimensionless shear rate $\dot{\gamma}\tau_0$.

The most surprising aspect of our predictions concerns the sharpness of the transition between weak and strong swelling as $\dot{\gamma}$ is increased. Indeed, within our dual-chain model, we predict a first-order stretching transition, whenever $n_b \gtrsim 4$. This is associated with a discontinuous jump in the fraction f of dragged chains. In the limit $n_b \gg 1$, this leads to a picture where an infinitesimal applied shear flow would pick out very few chains (a fraction $f \sim n_b^{-2}$) and drag them significantly, leaving the remainder undisturbed. Of course, in this limit, one should be concerned about possible non-linear behaviour associated with the finite extensibility of the coils. Nevertheless, the result is an interesting one since if this instability is present in our dual-chain model, it may well be present also in a more detailed theory based on a parabolic brush profile (based on a continuous and self-adjusting distribution of chain ends within the brush). Obviously, this would imply, for large n_b, a very strong breakdown of the Alexander-de Gennes ansatz (that all chains behave alike) under flow conditions. Further efforts toward a fully self-consistent theory of brushes under shear would therefore be of urgent interest.

3. Detachment of a Grafted Chain Under Shear Flows

We now turn to the question of the desorption of individual grafted chains in a brush submitted to a shear flow. We examine this process in the context of our dual-chain model for brush

deformation and we focus on one chain belonging to the upper dragged layer. As argued below, the detachment process is hastened by putting the chain under extra tension. Hence, we expect that the global rate of chain desorption from the brush is dominated by the contribution of the dragged chains rather than the quiescent ones. We first consider the case of a compact end-sticker and then the case of diblock copolymers grafted *via* an insoluble block. Note that in this section lengths are *not* in units of L_0.

Desorption of one chain initially attached by a compact end-sticker to a surface supporting an equilibrium brush has been recently studied by Wittmer *et al.* [15]. Their results for Rouse chains in good solvent conditions indicate that the release of one chain can be interpreted in terms of a two step process. First, the sticker must detach from the grafting surface and escape from a potential well of depth of order k_BT by diffusing a distance of the order of ξ_0, the size of the first blob for equilibrium brushes (also the mean distance between two grafted chains). Once the end-sticker has moved ξ_0 away from the grafting surface, the motion becomes deterministic and the chain is expelled from the brush by a net force due to chain tension and osmotic pressure effects. The crucial point is that the limiting step is the first one, and hence that the rate of desorption may then be written in the form

$$\mathcal{R}_{eq} \cong \frac{1}{\tau_{eq}} \exp\left[-\Delta U/k_BT\right] \tag{12}$$

where τ_{eq} is the characteristic time for the unbound sticker to reach the other side of the first blob, and ΔU is the effective barrier height. Equation (12) indicates that desorption is dominated by a local process, independent of N, which is related to the dynamics of the first blob.

One possible estimation for this time is $\tau_{eq} = \tau_0$, the characteristic relaxation time of the blob, and, indeed, the results of reference [15] for Rouse chains are in rough agreement with this choice. We note, however, that this is certainly not a trivial assumption since τ_{eq} is associated with the diffusion of one end through the first blob, rather than the relaxation of the blob itself. For Zimm chains, this choice for τ_{eq} in equation (12) leads to $\mathcal{R}_{eq} \sim \xi_0^{-3}$. The underlying physics of the equilibrium desorption process studied in reference [15] is that neighbouring blobs do not play a significant role in the initial stage of the detachment process; the characteristic length is that of a section of chain storing k_BT of stretching energy, *i.e.* the Pincus blob size [18]. We may generalize this approach to sheared layers by using the appropriate Pincus blob size $\xi_\uparrow$ in equation (12), leading to

$$\frac{\mathcal{T}}{\mathcal{T}_{eq}} = \frac{\mathcal{R}_{eq}}{\mathcal{R}} \cong \left(\frac{\xi_\uparrow(\dot{\gamma}\tau_0)}{\xi_0}\right)^3 \tag{13}$$

where $\mathcal{T}$ is the characteristic desorption time. An extra tension on the chain decreases $\xi_\uparrow$ and thus hastens the detachment. Within the Pincus scheme for a chain under tension, $\xi_\uparrow \sim L^{-3/2}$. Hence, the dependence of $\mathcal{R}/\mathcal{R}_{eq}$ on $\dot{\gamma}\tau_0$ is directly related to $L(\dot{\gamma}\tau_0)$, which may be deduced from the analysis of Section 2. Figure 6 shows plots of $\mathcal{T}/\mathcal{T}_{eq}$ *versus* $\dot{\gamma}\tau_0$, both for the case of our dual-chain model (for $n_b = 4, 5, 7$ and 10, solid curves) and for the Alexander-de Gennes limit of $f = 1$ (dashed curve). The dual-chain model results indicate an n_b-dependent and potentially sharp drop in the characteristic time $\mathcal{T}$ for $\dot{\gamma}\tau_0 \leq 0.2$, corresponding to the onset of strong brush swelling (cf. Fig. 5). The analogous $f = 1$ results show a more gradual drop in $\mathcal{T}$ occurring for $\dot{\gamma}\tau_0 \gtrsim 1.0$. These results suggest that an experiment which measures the rate of detachment as a function of shear rate and of n_b should be sensitive to the difference between our dual-chain model and the model of reference [10].

The case of diblock copolymers (polymers A grafted to the surface by an insoluble block of polymer B) is quite different. We presume that the solvent is good for polymer A and poor for

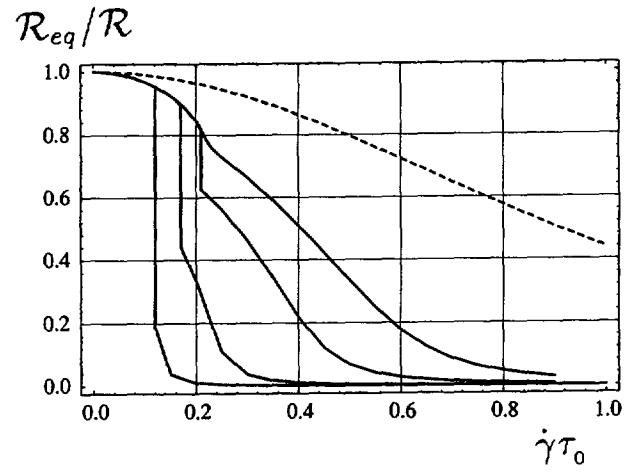

Fig. 6. — Plot of the inverse desorption rate $\mathcal{R}_{eq}/\mathcal{R}$ *versus* $\dot{\gamma}\tau_0$ for the dual-chain model for chains grafted by a compact end-sticker. The solid lines are for $n_b = 4$ (highest curve), 5, 7, and 10 (lowest curve), while the dashed line is for the case where we impose $f = 1$.

the anchor. In a simplified view, we assume that the B-chains form a dense, molten layer near the surface from which we may extract any of the anchoring blocks independently. Driving the junction between the A and B blocks into the solution results in a free energy cost due to partial exposure of the B-chain to a poor solvent. If the extracted B-chain is pictured as a string of collapsed molten blobs of size d, then assuming an energy of k_BT per blob gives $d \cong (k_BT/\Gamma)^{1/2}$, where Γ is the effective surface tension of the B-monomer/solvent interface. The energy of a string of such exposed blobs of length l then scales as

$$\mathcal{F}_{ch} \cong k_BT\frac{l}{d} \tag{14}$$

At equilibrium (zero-flow limit), this penalty is not compensated until $l \cong \xi_0$, when the last blob of the A block emerges from the layer and stored elastic energy in the A block begins to relax through the formation of a large coil protruding into the solvent region. Once $l > \xi_0$ the center of mass of the grafted chain is then driven out of the brush by a constant tension of order k_BT/ξ_0. Since in practice $d \ll \xi_0$, one always has $k_BT/\xi_0 \ll k_BT/d$. We thus only expect a small change in the slope of $\mathcal{F}_{ch}$ *versus* l until the B block anchor leaves the molten layer of B monomers. This occurs at $l = l_c \cong N_B d/(d/a)^3$, where N_B is the index of polymerization of the B-chains.

The presence of a shear field modifies this picture substantially (see Fig. 7). The idea is that the large blob which appears at the top of the layer during the detachment process is subject to hydrodynamic drag from the solvent flow. As the detachment process progresses, this blob is fed by the A-chain and increases its size. Thus, the hydrodynamic drag force on the chain also increases. The net result is that the chain is now driven out of the layer by an *increasing* tension.

The analysis of this process is greatly simplified by assuming that the tilt angle remains essentially constant during the expulsion [19]. With this simplification, the effective free energy of a detaching chain can be written in the form

$$\bar{\mathcal{F}}_{ch} \cong k_BT\frac{l}{d} + \mathcal{U}(l) \tag{15}$$

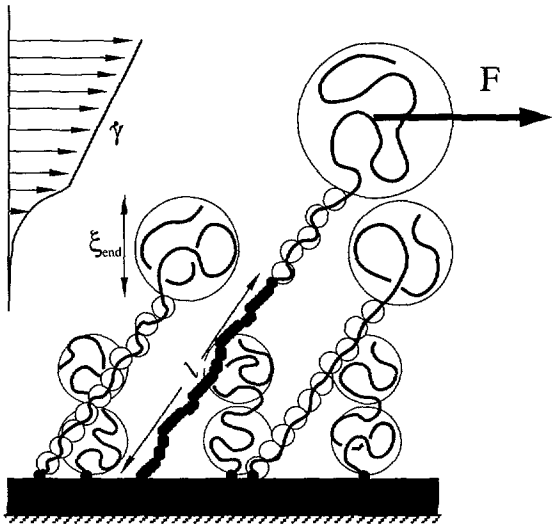

Fig. 7. — Sketch of the detachment of one diblock in a shear flow.

where $\mathcal{U}(l)$ represents the work done by the drag force during chain pull out. In the first stage of this process, $\mathcal{U}(l)$ can be written as

$$\frac{\mathcal{U}(l)}{k_B T} \cong -\left(\frac{d}{\xi_0}\frac{\dot{\gamma}\tau_0}{f}\sin\theta\right)\frac{l}{d} \qquad \text{for } l \leq \xi_{end} \tag{16}$$

where $\xi_{end} \cong \xi_0/f^{1/2}$ is the size of the large end-blob before the desorption process begins. As in the case of equilibrium desorption, this initial stage involves a free energy penalty which is linear in l, but with a reduced slope due to the work done by the hydrodynamic drag force. Once $l > \xi_{end}$, the end blob size becomes larger than ξ_{end}, scaling as $\tilde{\xi}_{end} \sim \xi_{end}\left(1 + (\xi_\uparrow/\xi_{end})^{5/3}(l - \xi_{end})/\xi_\uparrow\right)^{3/5}$ In this region, $\mathcal{U}(l)$ is rapidly dominated by the hydrodynamic drag on this new larger end blob and then has the form

$$\frac{\mathcal{U}(l)}{k_B T} \cong -\dot{\gamma}\tau_0 \sin\theta \left\{ f^{-11/6}\left(\frac{\xi_0}{\xi_\uparrow}\right)^{2/3}\left[\left(\frac{\tilde{\xi}_{end}}{\xi_{end}}\right)^{11/3} - 1\right] + f^{-3/2}\right\} \tag{17}$$

for $\xi_{end} \leq l \leq l_c$. In this equation, $\xi_{end} \cong \xi_0/f^{1/2}$ and l_c is the limiting length scale corresponding to complete B-chain pull out. Note that f, $\xi_\uparrow$ and θ in equations (16, 17) are functions of the shear rate determined by the analysis of Section 2.

Figure 8 shows the resulting potential $\bar{\mathcal{F}}_{ch}$ *versus* l for different values of $\dot{\gamma}\tau_0$; parameters are chosen so that $l_c/\xi_0 = 10$. Notice that the slope of the potential continuously decreases as soon as the shear rate is non-zero; however, at low shear rates the maximum value of $\bar{\mathcal{F}}_{ch}$ is still attained at $l = l_c$. At higher shear rates the position l_m of the maximum of $\bar{\mathcal{F}}_{ch}$ shifts away from l_c to a lower value corresponding to the point where $\partial\bar{\mathcal{F}}_{ch}/\partial l|_{l=l_m} = 0$. Using equations (15-17), gives in this regime

$$l_m \cong f^{-1/2}\xi_0 + \xi_\uparrow\left(\frac{f^{-1/2}\xi_0}{\xi_\uparrow}\right)^{5/3}\left[\left(\frac{f\xi_0}{\dot{\gamma}\tau_0 d\sin\theta}\right)^{5/6} - 1\right] \tag{18}$$

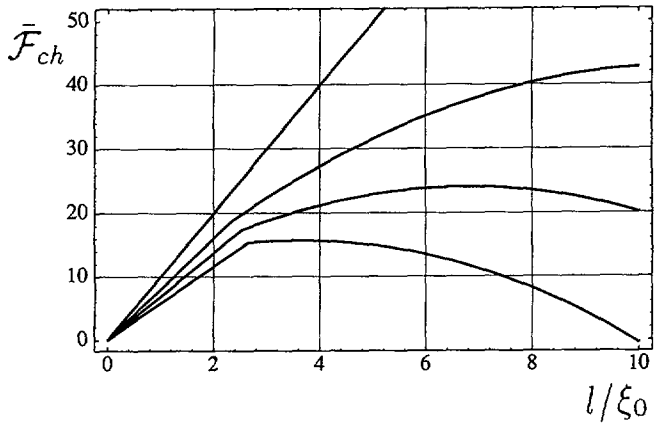

Fig. 8. — Plots of the free energy of one diblock $\bar{\mathcal{F}}_{\rm ch}$ *versus* l/ξ_0 for $\dot{\gamma}\tau_0$ =0.1 (highest curve), 0.5, 0.6, and 0.7 (lowest curve). (The parameters are $n_{\rm b} = 5$, $\xi_0/d = 10$ and $l_{\rm c}/\xi_0 = 10$ (see text).)

Finally, in the limit of large shear rates, the position $l_{\rm m}$ of the maximum value of $\bar{\mathcal{F}}_{\rm ch}(l)$ is pinned at $l_{\rm m} = \xi_{\rm end}$.

Since desorption is thermally activated, we may generally write the rate of desorption in terms of a Boltzmann factor as

$$\mathcal{R} \sim \exp\left[-\Delta\bar{\mathcal{F}}_{\rm ch}/k_{\rm B}T\right] \tag{19}$$

where $\Delta\bar{\mathcal{F}}_{\rm ch} = \bar{\mathcal{F}}_{\rm ch}(l_{\rm m})$ is a barrier height corresponding to the maximum of the curve $\bar{\mathcal{F}}_{\rm ch}(l)$. This may be calculated numerically in each of the three regimes described above and used in (19) to predict $\mathcal{R}$. It is interesting to compare the rates predicted in this way with equation (13) describing the compact end-sticker situation. In Figure 9, we show sample plots of $\mathcal{R}$ *versus* $\dot{\gamma}\tau_0$ for grafted copolymers (cf. Fig. 6 for compact end-stickers). In both cases the process of detachment of an initially grafted chain is hastened by shear flows and subject to the effects of discontinuous swelling for $n_{\rm b} \gtrsim 4$. (Clearly if f is discontinuous, then so is $\mathcal{R}$ in both cases.) But the behaviour beyond the swelling transition is quite different in the two cases. In the case of a compact end sticker, the prefactor of the exponential Boltzmann factor is affected, leading to a power-law dependence of the rate of detachment *versus* the shear rate. More precisely, in the limit $\dot{\gamma}\tau_0 \gg 1$, we have $(\dot{\gamma}\tau_0) \sim f(2-f)^{1/2}/(2-\tilde{h}_\perp^3)^{3/4}$ (Eq. (6)) and $L \sim (2-f)^{1/3}/(2-\tilde{h}_\perp^3)^{1/2}$ (Eq. (5)). Combining these, we find $\mathcal{R} \sim (\dot{\gamma}\tau_0)^3$. In the diblock situation, however, the height of the potential barrier itself is reduced by the shear flow and hence the detachment rate is exponentially decreased [20], the argument in the exponential being in general a non-trivial function of the shear rate. In the limit $\dot{\gamma}\tau_0 \gg 1$ however, this argument becomes a linear function of $\dot{\gamma}\tau_0$ and thus, roughly speaking, we expect $\mathcal{R} \sim \exp(\dot{\gamma}\tau_0)$.

This difference might be of some relevance in practical situations where the layer behaviour in shear flows has to be controlled. We have shown that for a given overall adsorption strength (given $n_{\rm b}$) a layer formed by end-attachment of stickers is more stable under shear than one made using diblock anchors. In physical terms, the tension arising from shear forces can lead to strong distortions of an anchor block (which adheres to the surface by many weak contacts) which promote desorption. The same force applied to a localized sticker has, in contrast, very little effect since the binding *force* is much stronger even for the same binding *energy*. This qualitative distinction is generic and does not depend strongly on our dual-chain model. Our

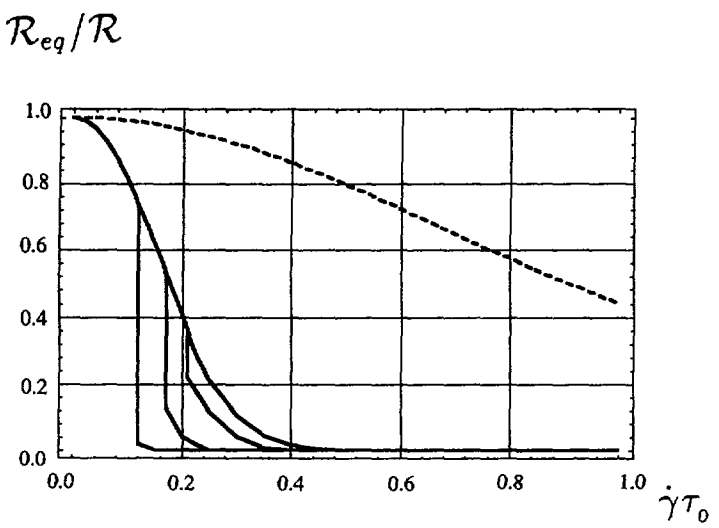

Fig. 9. — Plot of the inverse desorption rate $\mathcal{R}_{eq}/\mathcal{R}$ *versus* $\dot{\gamma}\tau_0$ for the diblock copolymer grafting mechanism ($n_b = 4$ (highest curve), 5, 7, and 10 (lowest curve)). The dashed line is for the case where we impose $f = 1$.

quantitative predictions of course do so and highlight the sensitivity of desorption to the state of the most strongly-stretched chains (see Figs. 8, 9).

4. Concluding Remarks

In this paper, we have considered a simple "dual-chain" model describing the behaviour of a polymer brush under shear flow. In this approach, two types of chain behaviour are allowed for the grafted chains: either they lie deep in the grafted layer, where the flow is screened, or they stretch under the action of the flow.

Qualitatively, we find two types of layer behaviour. At low shear rates, the majority of chains stretch while a minority are retracted into the quiescent region of the brush. At sufficiently high shear rates, however, the lowest possible fraction is exposed to the flow, while the majority remain screened from the flow. Quantitatively, we find a higher susceptibility of the brush to shear fields than is predicted in models based on the Alexander-de Gennes-type ansatz that all chains stretch alike (cf. Fig. 5). In particular, the onset of strong swelling occurs at a lower shear rate ($\dot{\gamma}\tau_0 \simeq 0.23$ rather than $\dot{\gamma}\tau_0 \cong 1$) and the asymptotic value of the relative swelling is somewhat larger. Although the numerical values are sensitive to prefactor uncertainties in the model, these trend are in rough agreement with experiments [3, 4]. Indeed, reference [3] reports measurements of the forces that act between surfaces bearing grafted polymer layers in good solvent as they slide past each other. These experiments show that above a certain threshold the normal forces between them become increasingly repulsive at higher velocities. This has been interpreted in terms of swelling of the layers and closing the gap that initially exists between them. Following this idea, in the situation designated as experiment (b) in reference [3], one has $\delta h \cong 0.24$ for $n_b \cong 8$ and $\dot{\gamma}\tau_0 \cong 0.37$. A theoretical estimate of δh based on a model where all chains would behave alike would give $\delta h \cong 0.02$, whereas in our model we would predict $\delta h \cong 0.35$. Although these are rough estimations, we see that the Alexander-de Gennes approach underestimates the response of the layer by one order of magnitude.

Furthermore, the transition between weak and strong swelling is also much sharper, becoming step-like for sufficiently long grafted chains. In fact, the onset of swelling and its asymptotic value can be mapped onto the results of reference [10] *via* (i) the "renormalization" of both the lengths and the shear rate, given in equations (9 11), and (ii) the knowledge of the variations of the fraction $f(\dot{\gamma}\tau_0)$ at a given n_b. These "renormalizations" shed some light on the nature of the higher susceptibility of the layer to solvent flows; the discontinuous swelling transition arises entirely through the f factor. Finally, the behaviour of the layer under shear fields is more strongly dependent on its static characteristics in our approach than in the previous studies [5,10] since not only the average size of the blob but also the average number of blobs per chain at equilibrium are crucially relevant for determining its response to shear flows.

Turning to chain desorption in shear flow, we have shown that desorption rate $\mathcal{R}$ is rather sensitive to flow, both for compact end-sticker and diblock copolymer grafting mechanisms (cf. Figs. 6 and 9). For the case of end-sticker grafting, we find at high flow rates a power-law dependence of $\mathcal{R}$ with $\dot{\gamma}\tau_0$. In the case of diblock grafting, we find that the barrier height is a strong function of shear rate, leading to an exponentially enhanced desorption rate. Thus, we expect that chain desorption from these two types of grafted layers would be very different experimentally. Other predictions for brush structure and grafted chain desorption could also be subjected to suitable experimental tests. Neutron reflectivity experiments could monitor brush structure under shear *in situ* and as a function of time. The results of Section 2 might be checked by measuring brush density profiles as a function of shear rate. In principle, the results of Section 3 on chain desorption might be tested by measuring the total surface coverage as a function of time and shear rate.

Clearly, however, our model is only a step towards a realistic theory of grafted layers in flow, and the numerical values that we get (which depend on many order-unity prefactors suppressed in our model) are only indicative [21]. An immediate improvement would be to relax the Alexander-de Gennes ansatz for the lower quiescent chains [22]. However, we do not expect that this would result in profound modifications of the behaviour of the system, since the Alexander-de Gennes picture is known to be a fairly good description for the properties of quiescent grafted chains. A fully self-consistent model would allow an arbitrary number of chain behaviours rather than just two. Although desirable, this is beyond reach for the moment. However, the scenario presented is quite rich and we believe that aspects of it (such as the first order swelling behaviour) might survive in a full treatment.

An interesting topic for future work is the study the influence of polydispersity on our results. It is unlikely that polydispersity should affect our scenario, but it is possible that this should smooth the first order type of transition that we get in the monodisperse case. This is because polydispersity induces a kind of length segregation of the tails [23]: the tails stretch away from the surface and then all the shorter chains will tend to have their free ends closer to the surface than that off any longer chain. Then, rather than performing a "discontinuous jump in f", the layer might choose to lower f by progressively retracting the shortest chains present in the upper layer until the final value of f is reached.

An other very interesting topic for future theoretical and experimental work is the study of the washing of a polymer brush. Indeed, our analysis suggests that the layer is globally less sensitive to the loss of a chain than expected from an Alexander-de Gennes-type brush. The idea is that the layer could react locally to the detachment of a chain by replacing it with a chain from the quiescent layer, leading to a replenishment of the upper layer. This mechanism is supported by the analysis of equation (10): if σ decreases, n_b decreases and thus f_{co} shifts to higher values. This implies that some initially quiescent chains are transferred to the upper layer.

Acknowledgments

We thank J. Wittmer and P. Pincus for very interesting discussions. This work was supported in part by the EPSRC and the DTI Colloid Technology Programme. One of us (M.A.) would like to thank N.A.T.O. for partial financial support.

References

[1] Milner S.T., *Science* **251** (1991) 905.
[2] Halperin A., Tirrell M. and Lodge T.P., *Adv. Polym. Sci.* **100** (1992) 33.
[3] Klein J., Perahia D. and Warburg S., *Nature* **352** (1991) 143.
[4] Klein J., *Colloids Surf. A* **86** (1994) 63.
[5] Barrat J.-L., *Macromolecules* **25** (1992) 832.
[6] Rabin Y. and Alexander S., *Europhys. Lett.* **13** (1990) 49.
[7] Alexander S., *J. Phys. France* **38** (1977) 983.
[8] de Gennes P.G., *J. Phys. France* **37** (1976) 1443; *Macromolecules* **13** (1980) 1069.
[9] Pincus P., *Macromolecules*, **9** (1976) 386.
[10] Harden J.L. and Cates M.E., *Phys. Rev. E*, submitted.
[11] Ajdari A., Brochard-Wyart F., de Gennes P.G., Leibler L., Viovy J.-L. and Rubinstein M., *Physica A* **204** (1994) 17; Rubinstein M., Ajdari A., Leibler L., Brochard-Wyart F., and de Gennes P.G., *C. R. Acad. Sci. Paris II* **316** (1993) 317.
[12] Brochard-Wyart F., *Europhys. Lett.* **23** (1993) 105.
[13] Milner S.T., Witten T.A. and Cates M.E., *Europhys. Lett.* **5** (1988) 413; *Macromolecules* **21** (1988) 2610.
[14] Skvortsov A.M., Gorbunov A.A., Pavlushkov I.V., Zhulina E.B., Borisov O.V. and Priamitsyn V.A., *Vysokomol. Soedin. A* **30** (1988) 1615; Zhulina E.B., Priamitsyn V.A. and Borisov O.V., *Vysokomol. Soedin. A* **31** (1989) 185.
[15] Wittmer J., Johner A., Joanny J.-F., Binder K., *J. Chem. Phys.* **101** (1994) 4379.
[16] Lapp A., Mottin M., Strazielle C., Broseta D., Leibler L., *J. Phys. II France* **2** (1992) 1247.
[17] This result can be recovered by setting $f = 1$ (or $f = 0$) and $\dot{\gamma} = 0$, and minimizing the pseudo-potential $\tilde{\mathcal{G}}$.
[18] For equilibrium layers, it happens that the Pincus blob size is equal to the mean distance between two grafted chains, but this is not true for brushes exposed to external perturbations.
[19] We can argue that two antagonistic effects play a role in fixing θ: for a given l, the elasticity favours low values of θ, whereas inclination is favoured by the drag force. We expect that these two effects offset each other, and hence we do not expect important variations of θ with l.
[20] We have not considered the prefactor in equation (19), but this might also be a function of the shear rate since the shape of the barrier is also affected by the flow, resulting in a small correction to our analysis.
[21] For example, more detailed versions of the dual-chain model give somewhat different numerical results but the same qualitative trends (*e.g.* evolution toward a state of "low f values" and thus enhanced layer susceptibility in flow); Aubouy M., Harden J.L. and Cates M.E., unpublished.
[22] Note that the resulting situation would probably be very similar to what was proposed by Johner and Joanny (*Europhys. Lett.* **15** (1991) 265) in the context of studying the "bridging" of two plates by grafted chains.
[23] Milner S.T., Witten T.A. and Cates M.E., *Macromolecules* **22** (1989) 853.